Z. Phys. C – Particles and Fields 50, 353–360 (1991)

Zeitschrift für Physik C Particles and Fields

A study of double pomeron exchange in $\pi^+ p$ and $K^+ p$ interactions at 250 GeV/c

EHS/NA22 Collaboration

M.R. Atayan[9], I.V. Ajinenko[7], Yu.A. Belokopytov[7], H. Böttcher[2], F. Botterweck[5], M.M. Chapkin[7], P.V. Chliapnikov[7], F. Crijns[5], A. De Roeck[1,a], E.A. De Wolf[1,b], K. Dziunikowska[3,c], A.M.F. Endler[6], Z.G. Garutchava[8], G.R. Gulkanyan[9], P. van Hal[5,d], T. Haupt[5,e], J.K. Karamyan[9], Z.A. Kirakosyan[9], D. Kisielewska[3,c], W. Kittel[5], S.S. Megrabyan[9], F. Meijers[5,f], A.B. Michałowska[1], I.V. Nikolaenko[7], K. Olkiewicz[3,c], V.M. Ronjin[7], A.M. Rybin[7], E.K. Shabalina[4], L. Scholten[5,g], O.G. Tchikilev[7], A.G. Tomaradze[8], L.A. Tikhonova[4], V.A. Uvarov[7], F. Verbeure[1], R. Wischnewski[2], S.A. Zotkin[4]

[1] Universitaire Instelling Antwerpen, B-2610 Wilrijk and Inter-University Institute for High Energies, VUB/ULB, B-1050 Brussels, Belgium
[2] Institut für Hochenergiephysik, O-1615 Berlin-Zeuthen, Federal Republic of Germany
[3] Institute of Physics and Nuclear Techniques of the Academy of Mining and Metallurgy and Institute of Nuclear Physics, PL-30055 Krakow, Poland
[4] Moscow State University, SU-117234 Moscow, USSR
[5] University of Nijmegen and NIKHEF-H, NL-6525 ED Nijmegen, The Netherlands
[6] Centro Brasileiro de Pesquisas Fisicas, 22290 Rio de Janeiro, Brazil
[7] Institute for High Energy Physics, SU-142284 Serpukhov, USSR
[8] Inst. of High Energy Physics of Tbilisi State University, SU-380086 Tbilisi, USSR
[9] Institute of Physics, SU-375036 Yerevan, USSR

Received 10 September 1990; in revised form 29 January 1991

Abstract. Quasi-elastic scattering with central dipion cluster production is studied in $\pi^+ p$ and $K^+ p$ interactions at 250 GeV/c. The cross section of double pomeron exchange is obtained as $\sigma_{\mathrm{DPE}}(\pi^+ p \to \pi^+(\pi^+\pi^-)p) = 24 \pm 5\,\mu\mathrm{b}$ and $\sigma_{\mathrm{DPE}}(K^+ p \to K^+(\pi^+\pi^-)p) = 19 \pm 5\,\mu\mathrm{b}$. The low energy pomeron-pomeron cross section is estimated for the first time.

1 Introduction

New direct information on the interaction properties of the pomeron and on its rôle in strong interaction physics can be extracted from the study of the processes in which it can be exchanged more than once. The simplest one among these is double pomeron exchange (DPE) [1–8]. This process is characterized by two fast leading hadrons (with Feynman $|x| > 0.9$) and a centrally produced diffractive cluster. Large rapidity gaps are required to isolate these central particles kinematically from the background. According to the existing literature (e.g. [5, 7]), this background is mainly due to single diffraction dissociation or pomeron-regge exchange.

DPE has recently been studied in pp-interactions at ISR energies (see Refs. in [7], and [9–12]). First results are now also available from the SPS collider [13]. In meson-nucleon scattering, attempts have been undertaken to study DPE in $K^+ p$-interactions at 70 GeV/c [14] and in $\pi^\pm p$-interactions at 147 GeV/c [15]. However, due to the small rapidity interval available, only upper limits for the DPE cross section could be obtained.

A better opportunity to study DPE in meson-nucleon scattering is given by the European Hybrid Spectrometer [16–18] at the CERN SPS exposed to a positive meson enriched beam with momentum 250 GeV/c. This momentum corresponds to a sufficiently large rapidity gap (7–8 units) between the colliding hadrons. A first study of the reactions

$$\pi^+ p \to \pi^+(\pi^+\pi^-)p, \tag{1}$$

$$K^+ p \to K^+(\pi^+\pi^-)p \tag{2}$$

at 250 GeV/c has been performed in [19] where an upper limit of the DPE process has been obtained.

In this paper we present our final results on the study of DPE in reactions (1) and (2). The experimental details are shortly described in Sect. 2. The estimate of the cross section and the study of the characteristics of the DPE process are presented in Sect. 3. An attempt to extract the low energy pomeron-pomeron cross section is undertaken in Sect. 4 and a summary is given in Sect. 5.

[a] Now at MPI, Munich, FRG
[b] Bevoegdverklaard Navorser NFWO, Belgium
[c] Partially supported by grants from CPBP 01.06 and 01.09
[d] Now with Ericsson Telecommunicatie B.V., Rijen, The Netherlands
[e] Now at Syracuse Univ., Syracuse, NY, USA
[f] Now at CERN, Geneva, Switzerland
[g] Now with PANDATA, Rijswijk, The Netherlands

2 Experimental details

The full experimental set-up of the European Hybrid Spectrometer (EHS) with the rapid cycling bubble chamber (RCBC) filled with H_2 as vertex detector is described in detail in [16–18]. Tracks of secondary charged particles are reconstructed from hits in the wire and drift chambers of the two lever arm spectrometer and from measurement in RCBC. The momentum resolution varies from (1–2)% for tracks reconstructed in the bubble chamber, to (1–2.5)% for tracks reconstructed in the first lever arm, and to 1.5% for tracks reconstructed in the full spectrometer.

Particle identification in EHS is supplied by RCBC, the Cerenkovs SAD and FC, the ionization sampling device ISIS and the transition radiation detector TRD.

Our results are based on 144220 $\pi^+ p$ events and 49564 $K^+ p$ events. The number of well measured and reconstructed 4-prong events with the proper charge balance and $\Delta p/p < 25\%$ for each track are equal to 9753 for $\pi^+ p$ and 3706 for $K^+ p$-interactions. The corresponding sensitivity, deduced from the results of [17], is 0.25 μb and 0.58 μb per event, respectively. The events are processed through the HYDRA kinematics program. We further select events with a χ^2-probability $P(\chi^2)$ for the 4C hypotheses (1) and (2) larger than 0.01% for which the leading particle in the c.m.s. forward hemisphere is a $\pi^+(K^+)$-meson with $x_{\pi^+}(x_{K^+}) > 0.9$ and the leading particle in the backward hemisphere is a proton with $|x_p| > 0.9$. These criteria lead to 83 events for reaction (1) and 35 events for reaction (2) all with, in fact, $P(\chi^2)$ $> 0.2\%$ for reaction (1) and $P(\chi^2) > 0.1\%$ for reaction (2). No event is found to simultaneously satisfy hypotheses (1) or (2) with a leading proton in the forward and with a leading pion (kaon) in the backward hemisphere, or a hypothesis with central $(K^+ K^-)$ or $(p\bar{p})$ instead of $(\pi^+ \pi^-)$-pair production.

We use the information on the identification of low-momentum ($p_{\text{lab}} < 1.2$ GeV/c) particles in RCBC and of centrally produced particles (with $p_{\text{lab}} < 20$ GeV/c) from the identification device ISIS, based on multiple sampling of the ionization [16]. We exclude events for which the leading backward particle is not consistent with the proton hypothesis and events for which at least one of the centrally produced particles cannot be accepted as a pion due to the χ^2 probability for the pion hypothesis being smaller than that for another hypothesis. The leading forward particle ($p_{\text{lab}} > 225$ GeV/c) is assigned the pion mass for reaction (1) and the kaon mass for reaction (2) for all events accepted. The number of events excluded is 10 for reaction (1) and 6 for reaction (2).

Events with low squared four momentum transfer to the quasi-elastically scattered meson ($|t_{\pi^+/K^+ \to (\pi^+/K^+)_f}| < 0.03$ GeV^2/c^2) have very low trigger efficiency and are excluded from further consideration. The remaining events are weighted to correct for losses induced by the interaction trigger [20]. The number of events remaining is 69 (or 128.8 weighted events) for reaction (1) and is 26 (or 45.6 weighted events) for reaction (2). Systematic errors due to this procedure are small compared to the statistical errors. The corresponding cross sections are

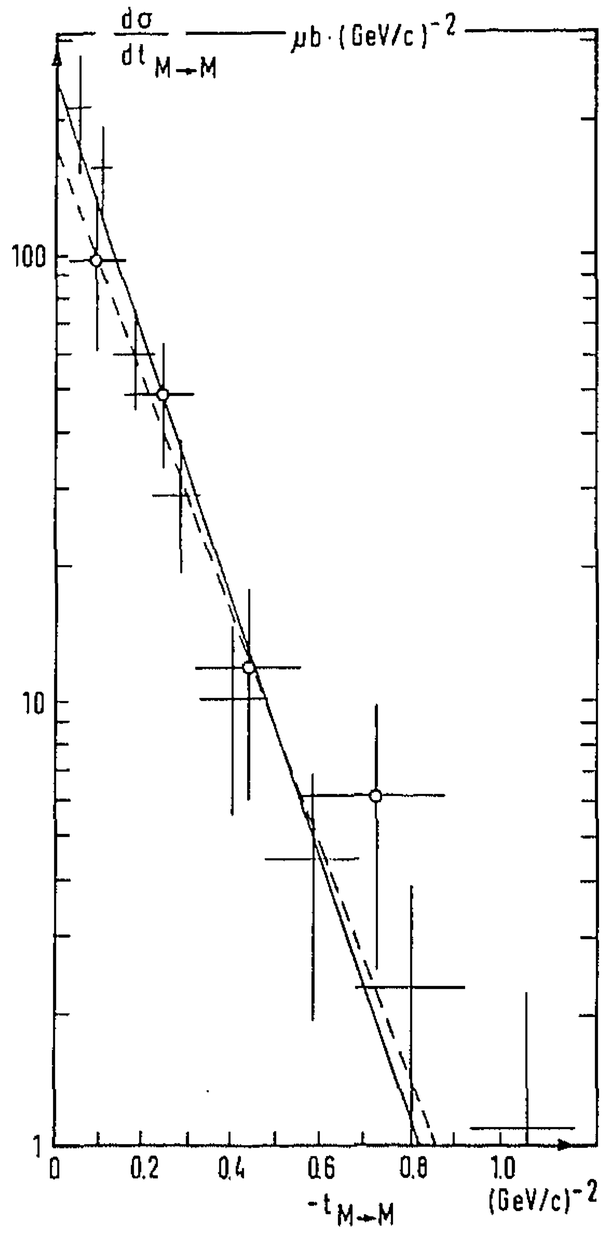

Fig. 1. Squared four-momentum transfer distribution $d\sigma/dt_{(\pi^+/K^+)\to(\pi^+/K^+)_f}$ for reactions (1) (crosses) and (2) (circles). The results of the exponential fits are also shown

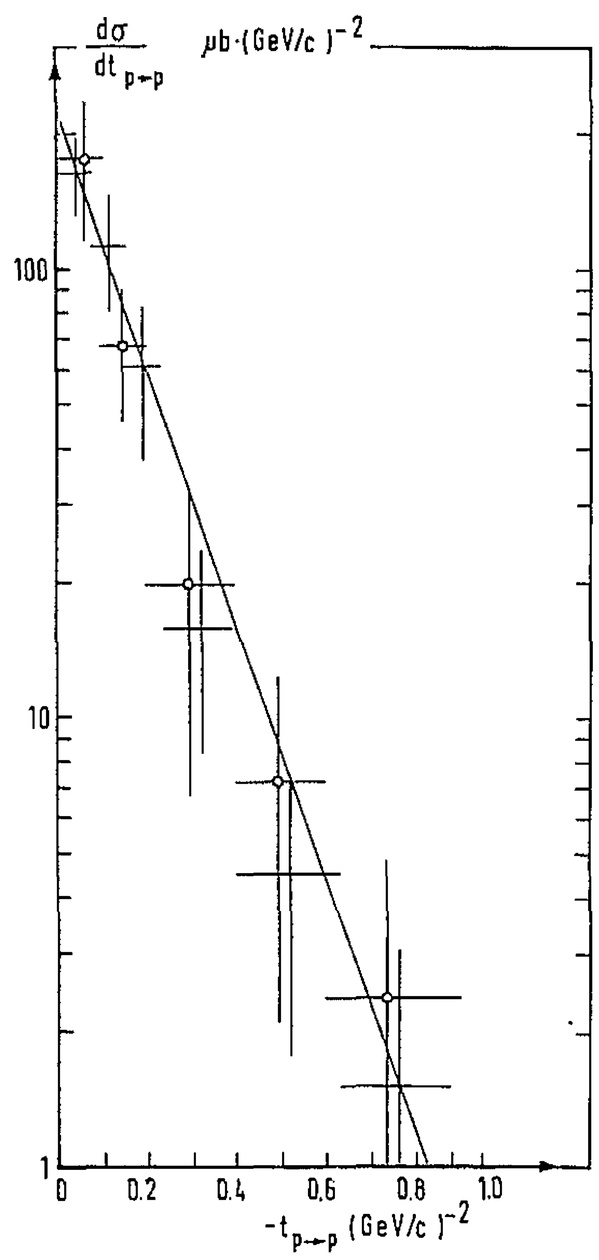

Fig. 2. Squared four-momentum transfer distribution $d\sigma/dt_{p\to p}$ for reactions (1) (crosses) and (2) (circles). The results of the exponential fit is also shown

$$\sigma'(\pi^+ p \to \pi_f^+ (\pi^+\pi^-) p) \begin{cases} x_p < -0.9 \\ x_{\pi_f^+} > 0.9 \\ |t_{\pi^+ \to \pi_f^+}| > 0.03\ (\mathrm{GeV/c})^2, \end{cases}$$
$$= 31 \pm 4\ \mu\mathrm{b}$$

$$\sigma'(K^+ p \to K_f^+ (\pi^+\pi^-) p) \begin{cases} x_p < -0.9 \\ x_{K_f^+} > 0.9 \\ |t_{K^+ \to K_f^+}| > 0.03\ (\mathrm{GeV/c})^2. \end{cases} \quad (3)$$
$$= 25 \pm 5\ \mu\mathrm{b}$$

The correction for the loss at $|t_{\pi^+/K^+ \to (\pi^+/K^+)_f}| < 0.03\ (\mathrm{GeV/c})^2$ is estimated from a fit of the experimentally observed spectra $\mathrm{d}\sigma/\mathrm{d}t_{\pi^+ \to \pi_f^+}$ and $\mathrm{d}\sigma/\mathrm{d}t_{K^+ \to K_f^+}$ (Fig. 1) by the exponential form $\sim b \exp[b(t+0.03)]$. The values of the slope parameter fitted by the maximum likelihood method are $b_\pi = (6.85 \pm 0.19)(\mathrm{GeV/c})^{-2}$ and $b_K = (5.98 \pm 0.34)(\mathrm{GeV/c})^{-2}$ for the π^+ and K^+ induced reaction, respectively. For $\mathrm{d}\sigma/\mathrm{d}t_{p \to p}$ (Fig. 2) we obtain $b_p = (7.29 \pm 0.26)(\mathrm{GeV/c})^{-2}$ for reaction (1) and $b_p = (6.66 \pm 0.40)(\mathrm{GeV/c})^{-2}$ for reaction (2), in good agreement with $b_p \approx 7\ (\mathrm{GeV/c})^{-2}$ obtained for the reaction $pp \to p(\pi^+\pi^-)p$ with quasi-elastically scattered protons and a centrally produced $(\pi^+\pi^-)$-cluster at $\sqrt{s} = 30.7$ GeV [21].

The corrected cross sections are

$$\sigma(\pi^+ p \to \pi^+ (\pi^+\pi^-) p) = 38 \pm 6\ \mu\mathrm{b} \begin{cases} x_p < -0.9 \\ x_{\pi_f^+} > 0.9, \end{cases}$$
$$\sigma(K^+ p \to K^+ (\pi^+\pi^-) p) = 29 \pm 6\ \mu\mathrm{b} \begin{cases} x_p < -0.9 \\ x_{K_f^+} > 0.9 \end{cases}. \quad (4)$$

The values (4) are close to those reported previously in [18], where only half of the present $\pi^+ p$ statistics was used, and can be considered as upper limits for the DPE cross section.

3 Cross section and characteristics of DPE

The rapidity y and Feynman-x distributions for the DPE candidates are shown in Figs. 3–4. With the x_f-cut on the leading particles, one obtains good rapidity separation of leading hadrons and centrally produced pions. However, even large rapidity gaps between leading and centrally produced hadrons do not necessarily exclude all non-pomeron exchanges. In particular, there could be a remnant of single diffraction dissociation, characterized by one of the exchanges being reggeon instead of pomeron.

However, it is expected that the background from single pomeron exchange (SPE) is different in the various phase space regions. This follows from a nonsimilar behaviour of the differential cross section for the pomeron-pomeron (PP), pomeron-reggeon (PR) and reggeon-pomeron (RP) exchange processes.

Below, the following variables will be used to describe the differential cross section:

$m_{\pi\pi}$ = the effective mass of the central cluster,
$t_1 = t_{p \to p}$,
$t_2 = t_{M \to M}$ (M denotes the leading meson: π^+ or K^+),

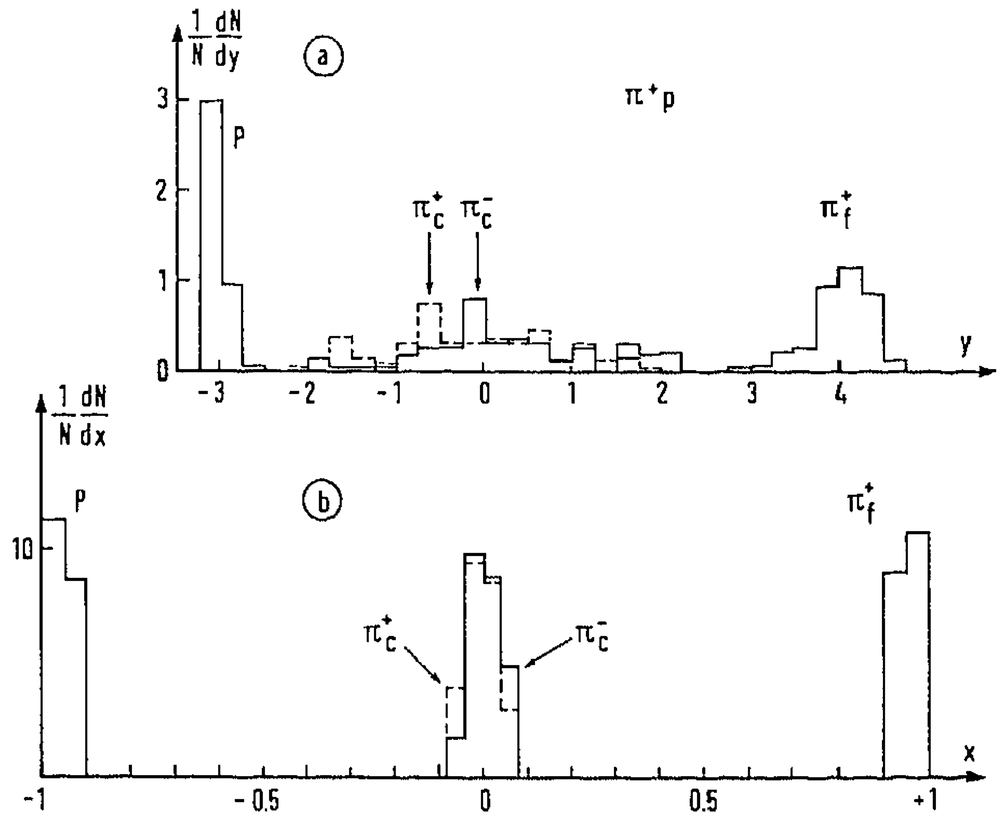

Fig. 3a, b. Rapidity y and Feynman-x distributions for reaction (1)

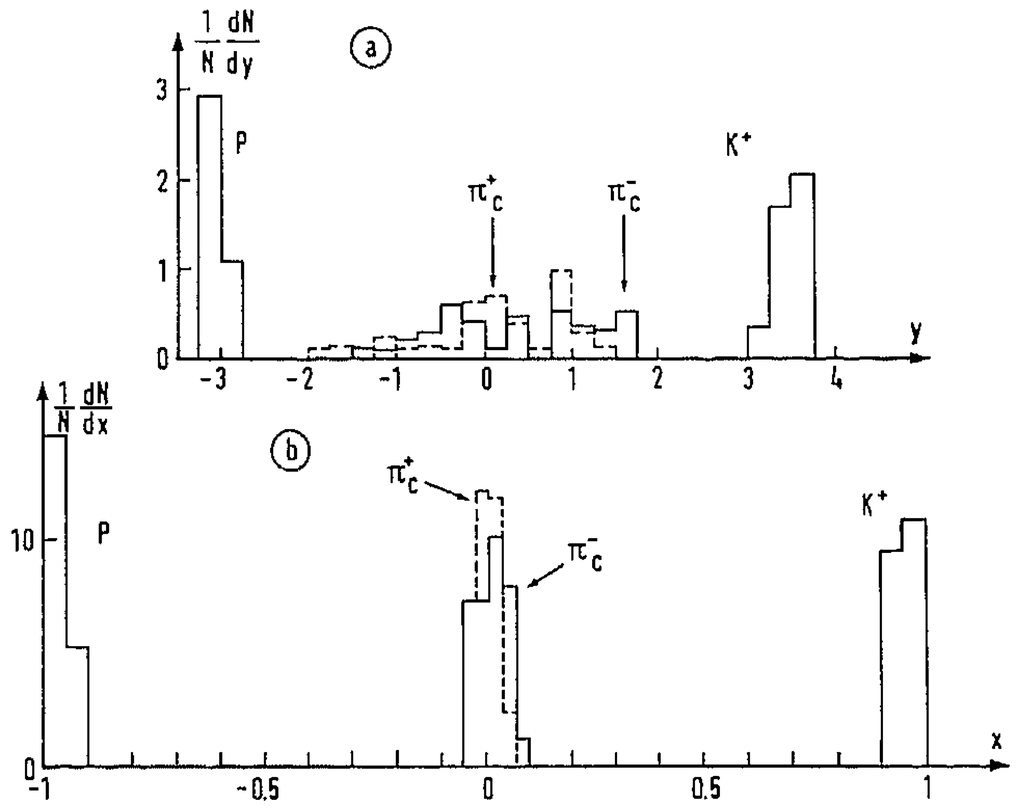

Fig. 4a, b. Rapidity y and Feynman-x distributions for reaction (2)

$z_1 = \ln(s/m^2_{p\pi\pi}) \approx \ln[1/(1-x_M)]$,
$z_2 = \ln(s/m^2_{M\pi\pi}) \approx \ln[1/(1-x_p)]$,

where s is the squared invariant energy of the meson-proton interaction ($\sqrt{s} = 21.7$ GeV), $m_{h\pi\pi}$ is the effective mass of leading hadron h and the centrally produced pions.

The invariant differential cross sections for the PP, PR and RP exchange processes (see Fig. 5) are [2, 6]

$$\frac{\mathrm{d}^4\sigma^{PP}}{\mathrm{d}t_1\,\mathrm{d}t_2\,\mathrm{d}z_1\,\mathrm{d}z_2} = \frac{1}{4}\sigma_{PP}(m^2_{\pi\pi}, t_1, t_2)\, g^2_{MP}(t_1)\, g^2_{pP}(t_2) \cdot \mathrm{e}^{2z_1(\alpha_P(t_1)-1)}\,\mathrm{e}^{2z_2(\alpha_P(t_2)-1)}, \quad (5a)$$

$$\frac{\mathrm{d}^4\sigma^{PR}}{\mathrm{d}t_1\,\mathrm{d}t_2\,\mathrm{d}z_1\,\mathrm{d}z_2} = \frac{1}{4}\sigma_{PR}(m^2_{\pi\pi}, t_1, t_2)\, g^2_{MP}(t_1)\, g^2_{pR}(t_2) \cdot \mathrm{e}^{2z_1(\alpha_P(t_1)-1)}\,\mathrm{e}^{2z_2(\alpha_R(t_2)-1)}, \quad (5b)$$

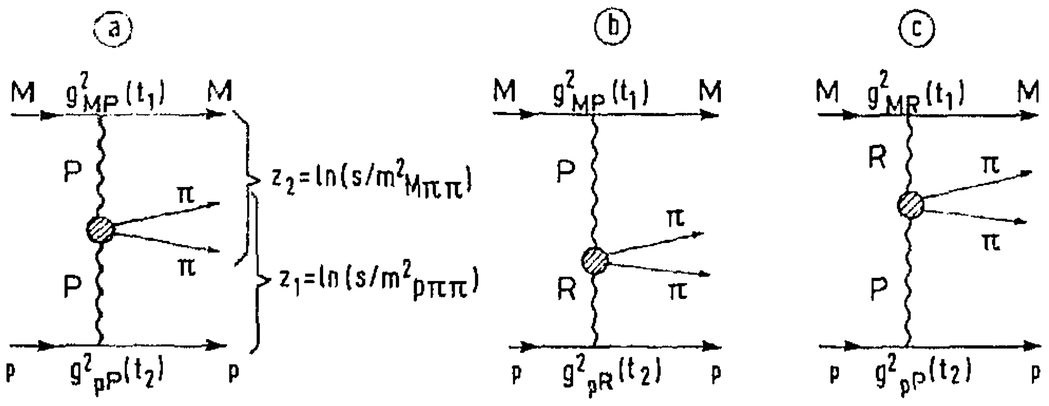

Fig. 5. Diagrams for **a** pomeron-pomeron, **b** pomeron-reggeon and **c** reggeon-pomeron exchange processes

$$\frac{d^4\sigma^{RP}}{dt_1\,dt_2\,dz_1\,dz_2}=\frac{1}{4}\sigma_{RP}(m^2_{\pi\pi},t_1,t_2)\,g^2_{MR}(t_1)\,g^2_{pP}(t_2)\cdot e^{2z_1(\alpha_R(t_1)-1)}e^{2z_2(\alpha_P(t_2)-1)}, \tag{5c}$$

where $\alpha_P(t)=1+\alpha'_P t$ is the pomeron trajectory and α'_P is its slope, $\alpha_R(t)=\frac{1}{2}+\alpha'_R t$ is the reggeon trajectory with intercept equal $\frac{1}{2}$ and slope α'_R. The functions $g^2_{hP}(t)$, $g^2_{hR}(t)$ describe the pomeron-hadron and reggeon-hadron couplings (see Fig. 5) and are parametrized as

$$g^2_{hP}(t)=g^2_{hP}(0)\,e^{R^2_{hP}t}, \tag{6a}$$

$$g^2_{hR}(t)=g^2_{hR}(0)\,e^{R^2_{hR}t}. \tag{6b}$$

The functions $\sigma_{PP}(m^2_{\pi\pi},t_1,t_2)$ and $\sigma_{PR(RP)}(m^2_{\pi\pi},t_1,t_2)$ define the pomeron-pomeron and pomeron-reggeon cross sections. They can depend on the "masses" t_1 and t_2 of the pomerons (reggeons); in this case we shall use the parametrization

$$\sigma_{PP}(m^2_{\pi\pi},t_1,t_2)=\sigma_{PP}(m^2_{\pi\pi},0)\,e^{R^2_0(t_1+t_2)}, \tag{7a}$$

$$\sigma_{PR}(m^2_{\pi\pi},t_1,t_2)=\sigma_{PR}(m^2_{\pi\pi},0)\,e^{r^2_0(t_1+t_2)}, \tag{7b}$$

with $\sigma_{PP}(m^2_{\pi\pi},0)$, $\sigma_{PR}(m^2_{\pi\pi},0)$, R^2_0 and r^2_0 as open parameters. This parametrization is the simplest and most convenient one. It allows to integrate (5) and to obtain (8) and (15). The distribution in t_1 and t_2 (Figs. 1 and 2) are described well by the exponential form. If the pomeron-pomeron interaction itself proceeds via one-pion exchange, with the usual pion-pomeron coupling $g^2_{\pi P}(q^2)=g^2_{\pi P}(0)\exp(R^2_{\pi P}q^2)$, this leads to $\sigma_{PP}(m^2_{\pi\pi},t_1,t_2)=\sigma(m^2_{\pi\pi},0)\exp R^2_\pi[(t_1+t_2)]$ which is just a special case of (7). Hitherto, no data exist on the parameters of expression (7a) characterizing the pomeron-pomeron interaction at low energies.

Note that in (5) the contribution of double reggeon (RR) exchange is omitted. Due to the small mass $m_{\pi\pi}$ of the central pion cluster (see below), (RR) is suppressed relative to DPE by a factor $(m^2_{\pi\pi}/s)\sim 10^{-4}-10^{-3}$. Furthermore, possible interference of DPE and SPE diagrams is ignored.

Integrating (5) over t_1 and t_2 one obtains:

$$\frac{d^2\sigma^{PP}}{dz_1\,dz_2}=\frac{1}{4}g^2_{MP}(0)\,g^2_{pP}(0)\,\sigma_{PP}(m^2_{\pi\pi},0)\cdot\frac{1}{(2\alpha'_P z_1+R^2_{MP}+R^2_0)(2\alpha'_P z_2+R^2_{pP}+R^2_0)}=\sigma_{PP}(m^2_{\pi\pi},0)\,f_{PP}(z_1,z_2), \tag{8a}$$

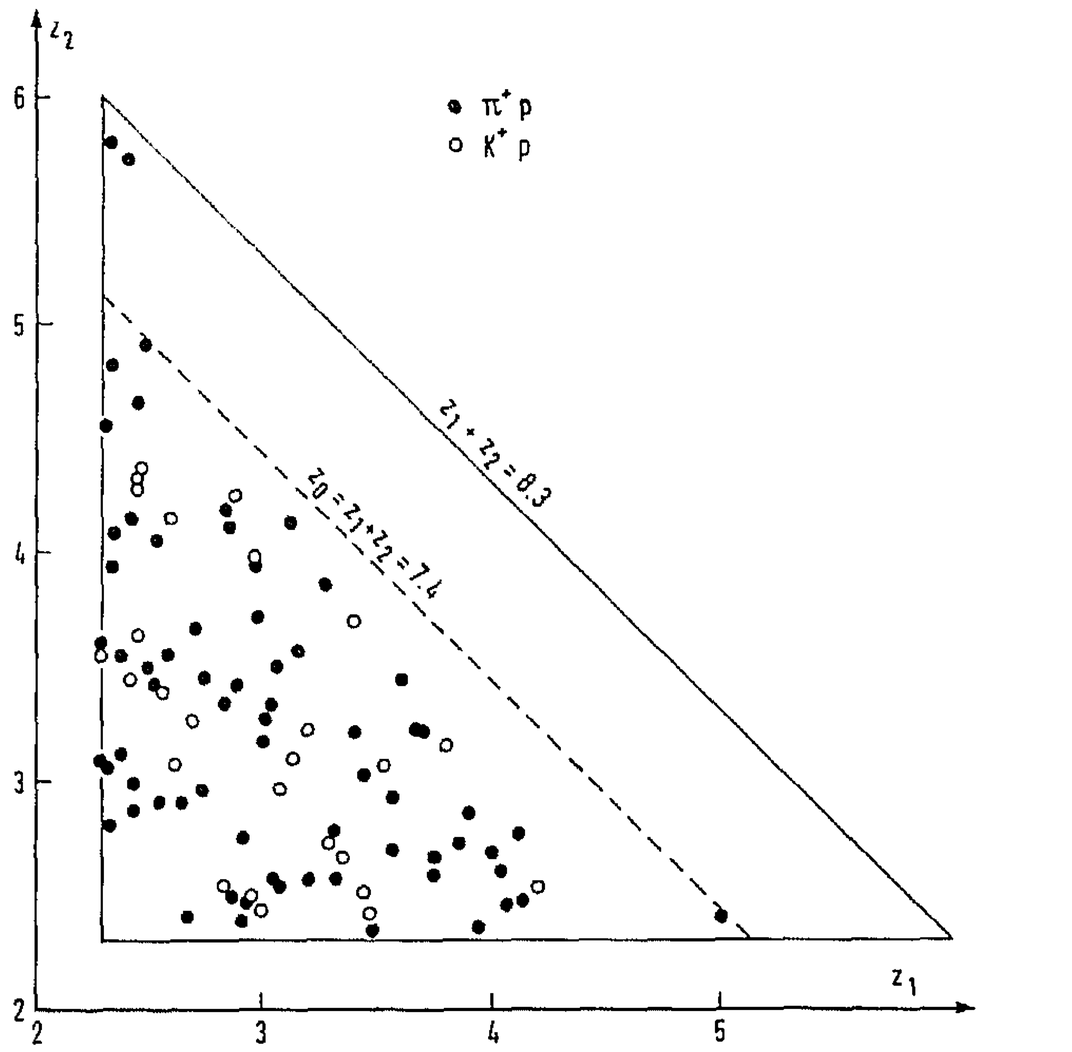

Fig. 6. Scatter-plot in the variables (z_1, z_2). Full circles correspond to reaction (1), empty circles to reaction (2)

$$\frac{d^2\sigma^{PR}}{dz_1\,dz_2}=\frac{1}{4}g^2_{MP}(0)\,g^2_{pR}(0)\,\sigma_{PR}(m^2_{\pi\pi},0)\cdot\frac{e^{-z_2}}{(2\alpha'_P z_1+R^2_{MP}+R^2_0)(2\alpha'_R z_2+R^2_{pR}+r^2_0)}=\sigma_{PR}(m^2_{\pi\pi},0)\,f_{PR}(z_1,z_2), \tag{8b}$$

$$\frac{d^2\sigma^{RP}}{dz_1\,dz_2}=\frac{1}{4}g^2_{MR}(0)\,g^2_{pP}(0)\,\sigma_{PR}(m^2_{\pi\pi},0)\cdot\frac{e^{-z_1}}{(2\alpha'_R z_1+R^2_{MR}+r^2_0)(2\alpha'_P z_2+R^2_{pP}+R^2_0)}=\sigma_{PR}(m^2_{\pi\pi},0)\,f_{RP}(z_1,z_2). \tag{8c}$$

For a limited interval of $m_{\pi\pi}$, where one can neglect the variation of σ_{PP} and σ_{PR}, DPE (8a) predicts only little variation of the density distribution in (z_1, z_2), while SPE ((8b) or (8c)) leads to exponentially decreasing distributions in z_1 or z_2.

The experimentally observed (z_1, z_2) distribution and its kinematical boundaries ($z_1, z_2 > z_{\min}\approx 2.3$ and $z_1+z_2<\ln(s/4m^2_\pi)\approx 8.3$) are shown in Fig. 6. The region of $z_1+z_2>z_0=7.4$ corresponds to very low dipion mass (note that $z_1+z_2=\ln(s/m^2_{\pi\pi\perp})$, were $m_{\pi\pi\perp}$ is the dipion transverse mass; for $z_1+z_2>7.4$, $m^2_{\pi\pi\perp}<0.28\,(\mathrm{GeV}/c^2)^2$), for which σ_{PP} and σ_{PR} are suppressed due to small phase space for the $\pi\pi$ system. In the region $z_1+z_2<z_0$, indeed, no strong variation of density is observed. This means, on the one hand, that SPE processes do not play a dominant role, and on the other, that σ_{PP} does not depend significantly on $m^2_{\pi\pi}\sim m^2_{\pi\pi\perp}=s\cdot\exp[-(z_1+z_2)]$.

In order to estimate the contribution from SPE, we therefore ignore the possible dependence of σ_{PP} and σ_{PR} on $m_{\pi\pi}$ in the region of $z_1+z_2<z_0$, and fit the one-

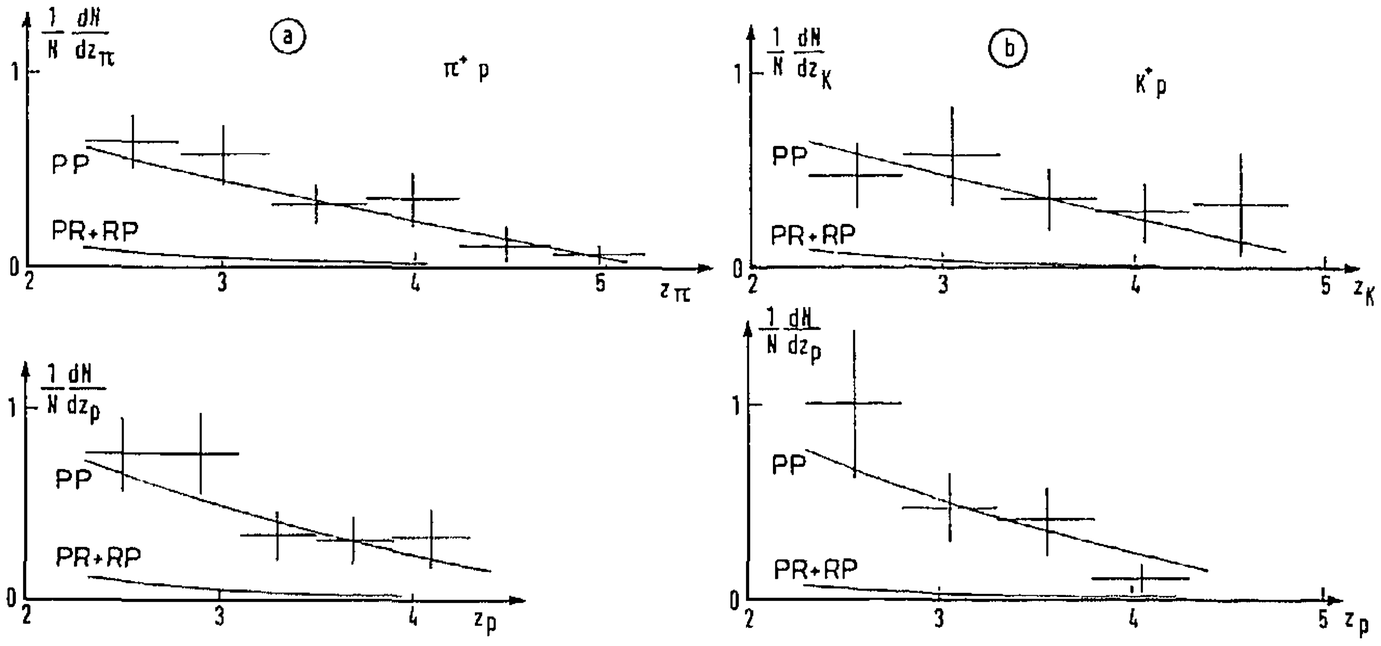

Fig. 7a, b. Distribution in the variables z_1 and z_2 for **a** reaction (1) and **b** reaction (2)

dimensional distributions in z_1 and z_2 (Fig. 7) by the expressions

$$d\sigma/dz_1 \sim \int_{z_{min}}^{z_0 - z_{min}} \{f_{PP}(z_1, z_2) + c_R[f_{PR}(z_1, z_2) + f_{RP}(z_1, z_2)]\} dz_2, \quad (9a)$$

$$d\sigma/dz_2 \sim \int_{z_{min}}^{z_0 - z_{min}} \{f_{PP}(z_1, z_2) + c_R[f_{PR}(z_1, z_2) + f_{RP}(z_1, z_2)]\} dz_1, \quad (9b)$$

with c_R characterizing the SPE contribution as a free parameter.

The parameters entering into the functions f_{PP}, f_{PR}, f_{RP} (see (8)) are taken from [6, 8, 22, 23]. The following values are used (all parameters are in units $(\mathrm{GeV/c})^{-2}$):

$$\begin{aligned}
&\alpha'_P = 0.2 \div 0.4, \quad \alpha'_R = 0.7 \div 1;\\
&g^2_{pP}(0) = 4, \quad g^2_{\pi P}(0) = 1.4, \quad g^2_{KP}(0) = 1.1;\\
&g^2_{pR}(0) = 1 \div 3, \quad g^2_{\pi R}(0) = 0.8 \div 1.2, \quad g^2_{KR}(0) = 0.2 \div 0.6;\\
&R^2_{pP} = 3.5 \div 4, \quad R^2_{\pi P} = 1.4 \div 2, \quad R^2_{KP} = 0.74 \div 1.24;\\
&R^2_{pR} = 7.1, \quad R^2_{\pi R} = 2, \quad R^2_{KR} = 3.1; \qquad (10)
\end{aligned}$$

R_0^2 and r_0^2 varies from 0 (where σ_{PP} and σ_{PR} are assumed to have a negligible dependence on t_1 and t_2) to $R_0^2 = R^2_{\pi P}$ and $r_0^2 = R^2_{\pi R}$ (where the PP and PR interactions occur via one-pion exchange). We have verified, that the choice of different sets of these parameters leads to different values of c_R, but practically has no influence on the integrated contribution of SPE in (9).

The combined fit of the $\pi^+ p$ and $K^+ p$ data (assuming the same c_R for both) shows that the contribution from SPE to the cross section in the considered region is small (see Fig. 7), but determined with large errors, $(15^{+30}_{-15})\%$ for $\pi^+ p$ and $(10^{+25}_{-10})\%$ for $K^+ p$-interactions. Subtracting these contributions, one obtains for $|t_1| > 0.03\ \mathrm{GeV}^2/c^2$:

$$\begin{aligned}
&\sigma'_{\mathrm{DPE}}(\pi^+ p \to \pi^+ (\pi^+ \pi^-) p) = 26^{+6}_{-10}\ \mu\mathrm{b},\\
&\sigma'_{\mathrm{DPE}}(K^+ p \to K^+ (\pi^+ \pi^-) p) = 22^{+5}_{-8}\ \mu\mathrm{b}. \qquad (11)
\end{aligned}$$

Another estimate of the DPE cross section can be obtained with the help of the rapidity gap method [4, 5, 24]. It can be shown that the rapidity gap $\Delta_{1(2)}$ between hadron $h_{1(2)}$ and the nearest centrally produced pion $\pi_{1(2)}$ is of very similar value as $z_{1(2)}$, and the distribution in $\Delta_{1(2)}$ is qualitatively similar to that in $z_{1(2)}$. In the case that a reggeon is exchanged between hadron $h_{1(2)}$ and the nearest pion $\pi_{1(2)}$, the distribution in $\Delta_{1(2)}$ is expected to have a rapidly falling form (see (8c) or (8b), and [5]). One can assume that the largest "arm" of the rapidity gap $\Delta_{\max} = \max(\Delta_1, \Delta_2)$ corresponds to pomeron exchange, and the smallest one $\Delta_{\min} = \min(\Delta_1, \Delta_2)$ corresponds to pomeron (DPE) or reggeon exchange (SPE). The relative contribution of the latter should decrease as $\Delta_{\min}$ increases.

The distribution in $\Delta_{\min}$ is shown in Fig. 8 for the combined π^+ and K^+ data. Under simplifying assumptions (see [5]), the SPE contribution can be represented by $\sim e^{-\Delta_{\min}}(z_0 - 2\Delta_{\min})$. Assuming that at the lower values of $\Delta_{\min}$ the differential cross section $d\sigma/d\Delta_{\min}$ is completely determined by SPE, one can estimate an integral contribution in the region of $\Delta_{\min} > 2$ of $(9 \pm 3)\%$. Thus, the events with $\Delta_{\min} > 2$ (51 and 18 events for reactions (1) and (2), respectively) can be accepted as an almost pure sample of DPE events. After subtraction of the SPE contribution the corresponding DPE cross section at $|t_1| > 0.03\ \mathrm{GeV}^2/c^2$ is

$$\begin{aligned}
&\sigma''_{\mathrm{DPE}}(\pi^+ p \to \pi^+ (\pi^+ \pi^-) p) = 19 \pm 4\ \mu\mathrm{b},\\
&\sigma''_{\mathrm{DPE}}(K^+ p \to K^+ (\pi^+ \pi^-) p) = 16 \pm 4\ \mu\mathrm{b}. \qquad (12)
\end{aligned}$$

Within the large errors these values are consistent with estimates (11).

The correction for loss of events with low momentum transfer ($|t_1| < 0.03\ \mathrm{GeV}^2/c^2$) is carried out according to

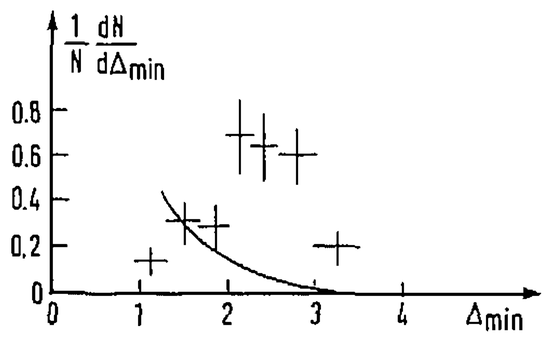

Fig. 8. Minimal rapidity gap distribution for the combined $\pi^+ p$ and $K^+ p$ data. The curve represents the SPE contribution parametrized as $\sim e^{-\Delta_{\min}}(z_0 - 2\Delta_{\min})$ and normalized at the point $\Delta_{\min} = 1.5$

Table 1. The mean characteristics of leading hadrons in the DPE

Reaction	Particle	$\langle x \rangle$	$\langle y \rangle$	$\langle \lvert t_{h\to h} \rvert \rangle$ $(\mathrm{GeV/c})^2$	$b(\mathrm{GeV/c})^{-2}$ (slope in $\mathrm{d}\sigma/\mathrm{d}t$)
(1)	p	-0.963 ± 0.003	-3.06 ± 0.02	0.15 ± 0.02	6.8 ± 0.6
	π_f^+	0.986 ± 0.004	4.03 ± 0.05	0.17 ± 0.03	7.3 ± 0.4
(2)	p	-0.967 ± 0.006	-3.09 ± 0.02	0.13 ± 0.04	7.8 ± 0.9
	K_f^+	0.938 ± 0.006	3.49 ± 0.04	0.20 ± 0.05	6.0 ± 0.7

Table 2. The mean characteristics of centrally produced pions in the DPE

Reaction	Particle (s)	$\langle x \rangle$	$\langle y \rangle$	$\langle p_T \rangle$ (GeV/c)	$\langle m_{\pi\pi} \rangle$ $(\mathrm{GeV/c^2})$
(1)	π_c^+	0.005 ± 0.004	0.17 ± 0.11	0.38 ± 0.03	
	π_c^-	0.016 ± 0.004	0.45 ± 0.12	0.33 ± 0.03	
	$(\pi^+\pi^-)_c$	0.021 ± 0.006	0.26 ± 0.08	0.52 ± 0.04	0.70 ± 0.04
(2)	π_c^+	0.013 ± 0.005	0.48 ± 0.13	0.32 ± 0.04	
	π_c^-	0.014 ± 0.007	0.29 ± 0.16	0.45 ± 0.04	
	$(\pi^+\pi^-)_c$	0.029 ± 0.010	0.36 ± 0.12	0.47 ± 0.05	0.73 ± 0.07

Table 3. The combined mean characteristics in DPE

Reaction	Combination	$\langle \Delta \rangle$	$\langle m_{h\pi_c} \rangle$ $(\mathrm{GeV/c^2})$
(1)	$(p\pi_c)_{\min}$	2.9 ± 0.1	2.98 ± 0.14
	$(\pi_f^+\pi_c)_{\min}$	3.2 ± 0.1	2.10 ± 0.16
	$p\pi_c^+$		3.44 ± 0.15
	$\pi_f^+\pi_c^-$		2.37 ± 0.16
(2)	$(p\pi_c)_{\min}$	3.1 ± 0.2	3.50 ± 0.15
	$(K^+\pi_c)_{\min}$	2.7 ± 0.1	1.94 ± 0.19
	$p\pi_c^+$		3.55 ± 0.20
	$K^+\pi_c^-$		2.88 ± 0.29

the method described in Sect. 2, with the help of the fitted slope parameters b_π and b_K for the DPE events of Table 1. The final values of the DPE cross sections are

$$\sigma_{\mathrm{DPE}}(\pi^+ p \to \pi^+(\pi^+\pi^-)p) = 24 \pm 5\ \mu\mathrm{b},$$
$$\sigma_{\mathrm{DPE}}(K^+ p \to K^+(\pi^+\pi^-)p) = 19 \pm 5\ \mu\mathrm{b}. \quad (13)$$

Average characteristics of the events with $\Delta_{\min} > 2$ (the almost pure sample of the DPE events) are shown in Tables 1–3. The characteristics of leading hadrons are presented in Table 1. The average rapidity gap between leading hadrons is 7.1 for reaction (1) and 6.6 for reaction (2). The slope parameters in the differential spectra $\mathrm{d}\sigma/\mathrm{d}t$ for DPE are consistent with those for the whole event sample.

The central pion characteristics are presented in Table 2. As can be seen from the last column, only low mass central clusters are produced ($\langle m_{\pi\pi} \rangle \sim 0.7\ \mathrm{GeV/c^2}$). They have comparatively large average transverse momentum ($\langle p_T \rangle_{\pi\pi} \sim 0.5\ \mathrm{GeV/c}$), low x ($\langle x_{\pi\pi} \rangle \sim 0.02 \div 0.03$) and rapidity ($\langle y_{\pi\pi} \rangle \sim 0.3$). The average transverse momentum of the centrally produced pions is approximately the same as that of pions produced in the central region of 4-prong non-single-diffractive $(\pi^+/K^+)p$-interactions at 250 GeV/c [25].

The average rapidity gap between the leading hadron and the nearest central pion (Table 3) is about 3 units. The average effective masses $\langle m_{\pi_f^+\pi_c^-} \rangle = 2.4$, $\langle m_{K_f^+\pi_c^-} \rangle = 2.9$ and $\langle m_{p\pi_c^+} \rangle \approx 3.5\ \mathrm{GeV/c^2}$ are far from the ρ^0, $K^0(890)$ and $\Delta^{++}(1232)$ masses, respectively, and it has been verified that no peaks are observed in the region of these resonances.

4 The pomeron-pomeron cross section

A first attempt is undertaken to extract information on the properties of the pomeron-pomeron interaction, itself. The unknown parameter R_0^2, which determines the dependence of the pomeron-pomeron cross section on the pomeron "masses" t_1 and t_2 in (7a), can be estimated from fitting the DPE data by the four-dimensional distribution (5a). A maximum likelihood fit is performed at fixed values of $\alpha'_P = 0.2$, 0.3 and 0.4, with as free parameters $R_1^2 = R_0^2 + R_{pP}^2$, $R_2^2 = R_0^2 + R_{\pi P}^2$ and $R_3^2 = R_0^2 + R_{KP}^2$. The mass dependence of $\sigma_{PP}(m_{\pi\pi}^2, 0)$ for the massless pomeron cross section (which is expected to be weak) is parametrized by the two-pion phase space dependence

$$\sigma_{PP}(m_{\pi\pi}^2, 0) \sim \sqrt{1 - 4m_\pi^2/m_{\pi\pi}^2}. \quad (14)$$

The results of the fit are given in Table 4 for the three values of α'_P. At given α'_P, three different estimates

Table 4. The fitted parameters R_1^2, R_2^2, R_3^2

α'_P $(\mathrm{GeV/c})^{-2}$	R_1^2 $(\mathrm{GeV/c})^{-2}$	R_2^2 $(\mathrm{GeV/c})^{-2}$	R_3^2 $(\mathrm{GeV/c})^{-2}$	R_0^2 $(\mathrm{GeV/c})^{-2}$
0.2	5.7 ± 0.5	4.6 ± 0.4	3.7 ± 0.7	2.4 ± 0.4
0.3	5.0 ± 0.5	4.0 ± 0.4	3.1 ± 0.7	1.9 ± 0.4
0.4	4.3 ± 0.5	3.3 ± 0.4	2.4 ± 0.7	1.2 ± 0.4

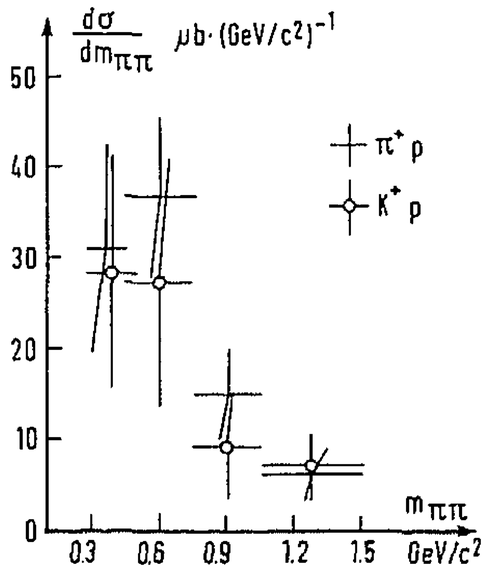

Fig. 9. Central cluster mass distributions for DPE in reactions (1) and (2)

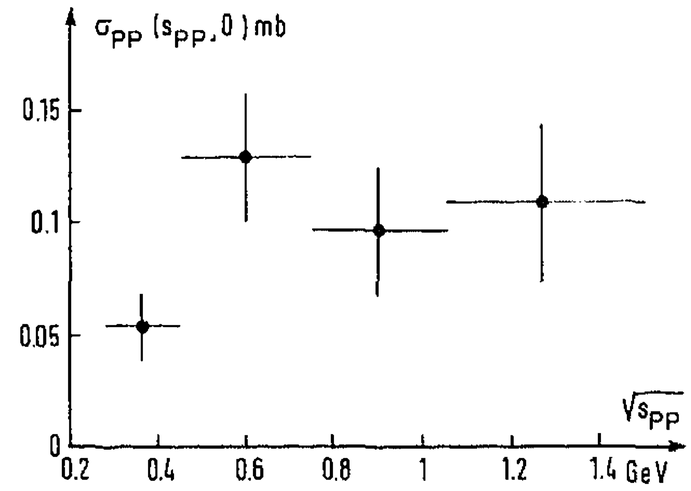

Fig. 10. Cross section for the massless pomeron interaction

of R_0^2 are obtained by subtracting from the fitted values of R_1^2, R_2^2 and R_3^2 the known "average" value of $R_{pP}^2 = 3.8 \pm 0.2$, $R_{\pi P}^2 = 1.7 \pm 0.3$ and $R_{KP}^2 = 1.0 \pm 0.2\,(\mathrm{GeV/c})^{-2}$, respectively (see Sect. 3). The three estimates of R_0^2 are consistent within errors and their average is given in the last column of Table 4.

At no value of α'_P, the obtained R_0^2 value is consistent with zero. Thus, the dependence of $\sigma_{PP}(m_{\pi\pi}^2, t_1, t_2)$ on t_1, t_2 cannot be ignored. The closeness of R_0^2 and $R_{\pi P}^2 (= 1.7 \pm 0.3\,(\mathrm{GeV/c})^{-2})$ may indicate that the one-pion exchange (OPE) between the two pomerons may play a significant rôle within the pomeron-pomeron interaction. However, this closeness is only a necessary, but not a sufficient condition. For additional information from the angular distribution see below.

The differential cross section $\mathrm{d}\sigma_{\mathrm{DPE}}/\mathrm{d}m_{\pi\pi}$ for reactions (1) and (2) is shown in Fig. 9. The theoretical expression for $\mathrm{d}\sigma_{\mathrm{DPE}}/\mathrm{d}m_{\pi\pi}$ can be deduced from (8a) and has the form [8]:

$$\frac{\mathrm{d}\sigma_{\mathrm{DPE}}}{\mathrm{d}m_{\pi\pi}} = \frac{g_{MP}^2(0)\, g_{pP}^2(0)}{8\alpha'_P \cdot m_{\pi\pi}} \cdot \frac{\sigma_{PP}(m_{\pi\pi}^2, 0)}{\alpha'_P \ln \dfrac{s}{m_{\pi\pi}^2} + \dfrac{R_{MP}^2 + R_{pP}^2 + 2R_0^2}{2}} \times \ln \frac{\left(2\alpha'_P \ln \dfrac{(1-x_m)s}{m_{\pi\pi}^2} + R_{MP}^2 + R_0^2\right)\left(2\alpha'_P \ln \dfrac{(1-x_m)s}{m_{\pi\pi}^2} + R_{pP}^2 + R_0^2\right)}{\left(2\alpha'_P \ln \dfrac{1}{1-x_m} + R_{MP}^2 + R_0^2\right)\left(2\alpha'_P \ln \dfrac{1}{1-x_m} + R_{pP}^2 + R_0^2\right)}, \quad (15)$$

where $x_m = 0.9$ is the Feynman x boundary of the leading hadron. From a comparison of the data and (15), the massless pomeron-pomeron cross section $\sigma_{PP}(m_{\pi\pi}^2, 0)$ is extracted. The results are found to be practically independent of the choice of parameter sets in Table 4 and coincide within errors for the $\pi^+ p$ and $K^+ p$ data. The dependence of $\sigma_{PP}(m_{\pi\pi}^2, 0)$ on $\sqrt{s_{PP}} = m_{\pi\pi}$ averaged over the $\pi^+ p$ and $K^+ p$ data is presented in Fig. 10. Above the rise at the two-pion threshold, $\sigma_{PP}(s_{PP}, 0)$ is consistent with being constant in the interval $0.45 < \sqrt{s_{PP}} < 1.5$ GeV. The cross section averaged over this interval is $\bar{\sigma}_0 = 0.11 \pm 0.02$ mb. Note, that in the quoted errors the possible uncertainty of the pomeron-hadron vertex parameters $g_{pP}^2(0)$, $g_{\pi P}^2(0)$, $g_{KP}^2(0)$ (which can reach 20%) is not included.

As the pomeron isospin is $T=0$, $\sigma_{PP}^{\pi^+\pi^-} = 2\sigma_{PP}^{\pi^0\pi^0}$ is expected. So the massless pomeron-pomeron total cross section (to two pions) is $\bar{\sigma}_0^{\mathrm{tot}} = 0.17 \pm 0.03$ mb at $\sqrt{s_{PP}} = 0.45 \div 1.5$ GeV and $\bar{\sigma}_0^{\mathrm{tot}} = 0.08 \pm 0.02$ mb at $\sqrt{s_{PP}} < 0.45$ GeV. These are first estimates of the low energy pomeron-pomeron cross section.

Our value for the massless pomeron-pomeron total cross section $\bar{\sigma}_0^{\mathrm{tot}} = 0.17 \pm 0.03$ mb for $0.45 < m_{\pi\pi} < 1.5$ GeV/c is in agreement with the theoretical prediction [8] for the high-energy limit $\sigma^{\mathrm{tot}}(s_{PP} \to \infty) \approx 0.14$ mb. Furthermore, some estimate for σ_{PP} can be extracted from [26], where the DPE contribution $\sigma_{\mathrm{DPE}}^{\mathrm{inv}}$ to the invariant cross section for the reaction $pp \to ppX$ is given. We extract $\sigma_0^{\mathrm{tot}}(m_{\pi\pi}^2, 0) = 0.48 \pm 0.07$ mb at $m_{\pi\pi} = 3.6\ \mathrm{GeV/c^2}$, noticeably larger than our estimate. This is probably due to the contribution from other channels, as $PP \to 4\pi, \to 2K$ etc.

Using the parametrizations (7) and (14) one can express the dependence of the total pomeron-pomeron cross section on their four-momenta q_1 and q_2 ($q_1^2 = t_1$, $q_2^2 = t_2$) as

$$\sigma_{PP}^{\mathrm{tot}}(q_1, q_2) = a\sqrt{1 - 4m_\pi^2/(q_1+q_2)^2}\, \exp\left[R_0^2(q_1^2 + q_2^2)\right] \quad (16)$$

with $a = (0.16 \pm 0.02)$ mb and $R_0^2 = (1.8 \pm 0.4 \pm 0.6)\,(\mathrm{GeV/c})^{-2}$, where the second error in R_0^2 is due to uncertainty in the pomeron slope α'_P.

The angular distribution of the centrally produced pions in the pomeron-pomeron frame is shown in Fig. 11. One can see that the angular distribution is con-

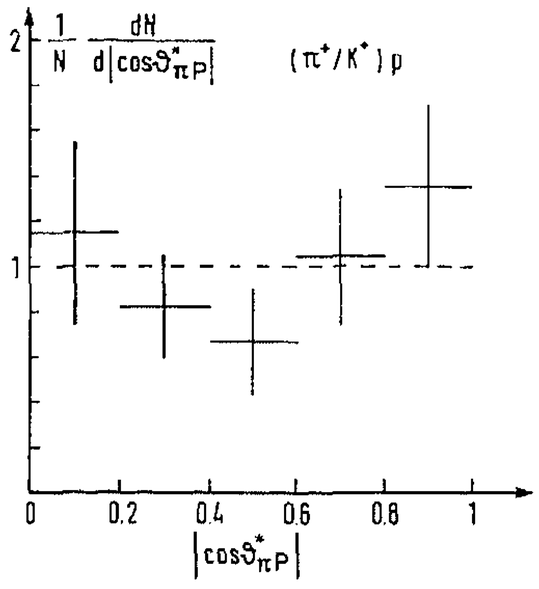

Fig. 11. Distribution in the cosinus of the angle between pomeron and pion in the pomeron-pomeron frame for DPE in reactions (1) and (2)

sistent with being isotropic, except for the low angle region. This means that the S-wave pomeron-pomeron interaction dominates. However, some contribution from the OPE mechanism (peaked at lower angles) cannot be excluded.

5 Summary

The reactions $\pi^+ p \to \pi^+(\pi^+\pi^-)p$ and $K^+ p \to K^+(\pi^+\pi^-)p$ with quasi-elastically scattered leading hadrons ($|x|>0.9$) and centrally produced pion pairs are studied at 250 GeV/c. It is shown that a dominant part of these reactions is consistent with the DPE process, and its cross section is obtained as

$$\sigma_{\mathrm{DPE}}(\pi^+ p \to \pi^+(\pi^+\pi^-)p) = 24 \pm 5\ \mu\mathrm{b},$$
$$\sigma_{\mathrm{DPE}}(K^+ p \to K^+(\pi^+\pi^-)p) = 19 \pm 5\ \mu\mathrm{b}.$$

For the first time estimates are obtained for the cross section of the massless pomeron interaction at low energies, $\bar{\sigma}_0^{\mathrm{tot}} = 0.17 \pm 0.03$ mb at $\sqrt{s_{pp}} = 0.45 - 1.5$ GeV and $\bar{\sigma}_0^{\mathrm{tot}} = 0.08 \pm 0.02$ mb at $\sqrt{s_{pp}} < 0.45$ GeV.

An approximate expression for the dependence of the pomeron-pomeron cross section on the four-momenta q_1 and q_2 is obtained as

$$\sigma_{PP}^{\mathrm{tot}}(q_1, q_2) = a\sqrt{1 - 4m_\pi^2/(q_1+q_2)^2}\,\exp\left[R_0^2(q_1^2+q_2^2)\right]$$

with $a = (0.16 \pm 0.02)$ mb and $R_0^2 = (1.8 \pm 0.4 \pm 0.6)$ $(\mathrm{GeV/c})^{-2}$.

Acknowledgements. It is a pleasure to thank the EHS coordinator L. Montanet and the operating crews and staffs of EHS, SPS and the H2 beam, as well as the scanning and measuring teams at our laboratories for their invaluable help with this experiment. One of the authors (G.G.) is grateful to G. Arakelyan and A. Grigoryan for helpfull discussions concerning the theoretical interpretation of our experimental data. We are grateful to III. Physikalisches Institut B, RWTH Aachen, Germany, University of Warsaw and Institute of Nuclear Problems Warsaw, Poland and Department of High Energy Physics, Helsinki University, Helsinki, Finland, for early contributions to this experiment.

References

1. D.M. Chew, G.F. Chew: Phys. Lett. 53 B (1974) 471
2. A.B. Kaidalov, K.A. Ter-Martirosyan: Nucl. Phys. B75 (1974) 471
3. D.M. Chew: Phys. Lett. 65 B (1976) 367
4. J. Pumplin, F.S. Henyey: Nucl. Phys. B117 (1976) 377
5. B.R. Desai, B.C. Shen, M. Jacob: Nucl. Phys. B142 (1978) 258
6. A.B. Kaidalov: Phys. Rep. 50 (1979) 157
7. G. Alberi, G. Goggi: Phys. Rep. 74 (1981) 1
8. K.H. Streng: Phys. Lett. 166 B (1986) 443
9. R. Waldi et al.: Z. Phys. C – Particles and Fields 18 (1983) 301
10. A. Breakstone et al.: Z. Phys. C – Particles and Fields 31 (1986) 185
11. A. Breakstone et al.: Z. Phys. C – Particles and Fields 40 (1988) 41
12. A. Breakstone et al.: Z. Phys. C – Particles and Fields 42 (1989) 387 and 48 (1990) 569
13. A. Brandt et al. (UA8): Observation of Double Pomeron Exchange Reaction at the SPS-Collider, Contribution to Singapore Conference, 1990
14. M. Barth et al.: Z. Phys. C – Particles and Fields 16 (1982) 111
15. D.H. Brick et al.: Z. Phys. C – Particles and Fields 19 (1983) 1
16. M. Aguilar-Benitez et al.: Nucl. Instr. and Meth. 205 (1983) 79
17. M. Adamus et al. (NA22): Z. Phys. C – Particles and Fields 32 (1986) 475
18. M. Adamus et al. (NA22): Z. Phys. C – Particles and Fields 39 (1988) 311
19. I.V. Ajinenko et al. (NA22): Z. Phys. C – Particles and Fields 43 (1989) 15
20. M. Adamus et al. (NA22): Phys. Lett. B186 (1987) 223
21. D. Drijard et al.: Nucl. Phys. B143 (1978) 61
22. L.A. Ponomarev: Part. Nucl. 15 (1976) 186
23. A.N. Kamalov, L.A. Ponomarev: Preprint ITEP-121 (1976)
24. M.-S. Chen, G.L. Kane: Phys. Lett. 60 B (1976) 192
25. I.V. Ajinenko et al. (NA22): Phys. Lett. 197 B (1987) 457
26. J.C.M. Armitage et al.: Phys. Lett. 82 B (1979) 143